The Korean Journal of Ceramics, **3** [3] 208 - 212 (1997)

Evaluation of Shear-Induced Phase Transformation of β-Cristobalite by Fiber Push-Out Technique

Sang-Jin Lee, Dong Zhu and Jae-Suk Sung*

Department of Materials Science and Engineering,
University of Illinois at Urbana-Champaign, Urbana, Illinois 61801, USA
**Korea Electronics Technology Institute, Pyungtaek, Kyunggi-Do, Korea*
(Received July 25, 1997)

Shear-induced phase transformation behavior of chemically stabilized β-cristobalite was studied by the fiber push-out technique. To obtain the critical grain size for phase transformation, the hot-pressed polycrystalline β-cristobalite, which was used as the interphase between fiber and matrix, was annealed at 1300°C for 10 h. Two types of fibers, mullite and sapphire fiber, were used in this study. Debonding between mullite fiber and cristobalite interphase occurred at a critical load of 230 MPa. Static friction and fiber sliding were continuously followed by debonding. Shear-induced transformation induced cracks in the cristobalite interphase at the debonding stage. In the case of the sapphire fiber, the debonding occurred at a lower load of 180 MPa due to the residual stress in the interface caused by the difference in thermal expansion coefficients between the fiber and the cristobalite interphase. The load was insufficient for shear-induced phase transformation.

Key words : Shear-induced transformation, β-cristobalite, Fiber push-out, Debonding

I. Introduction

"Phase transformation weakening" mechanisms of interphase materials have been recently introduced.[1-3] It has been proposed that debonding occurs at the weakened interphase in a laminated or fiber coating structure.[4-8] It can be achieved by inducing a displacive, crystallographic phase transformation, which is accompanied by a negative volume and/or unit cell shape change, thereby causing microcracks in the interphase. The dissipative energy associated with the transformation results in an overall increase in the toughness of the bulk composite. Enstatite[9] has been intensively researched as a transformation weakener. In recent, β-cristobalite (SiO_2)[10,11] was found to exhibit phase transformation weakening effects at room temperature.

β-cristobalite is a high temperature, low pressure polymorph of silica (SiO_2) in which the SiO_4 tetrahedra are arranged in a diamond-like lattice with shared corners.[12] The fully expanded, high temperature, β-structure undergoes a reversible displacive transformation to a collapsed α-structure on cooling at 265°C. This is accompanied by a volume decrease of approximately 3.2%.[13,14] In order to stabilize the β-cristobalite at room temperature, it can be chemically doped with "stuffing" cations.[15,16] In a chemically stabilized β-cristobalite, the presence of foreign ions in the interstices presumably inhibits the contraction of the structure. This normally occurs during the $\alpha \Leftrightarrow \beta$ cristobalite transformation. The chemically stabilized cristobalite has cubic (β form) rather than tetragonal (α form) symmetry after cooling.

A critical particle size effect is believed to control the β to α transformation in the metastable β-cristobalite analogous to the onset of nucleation in zirconia (ZrO_2)[17] and in some other silicates.[18-20] In a polycrystalline β-cristobalite, the grain size depended on densification temperature and annealing conditions. For polycrystalline β-cristobalite doped with Ca^{2+} and Al^{3+} cations, the critical grain size of 4~5 μm was required to transform to α-cristobalite.[11] The shear-induced transformed α-cristobalite was observed in the polycrystalline β-cristobalite after grinding.[11]

In this paper, the chemically stabilized β-cristobalite powder, synthesized by solution-polymerization technique using PVA solution as a polymeric carrier, was densified by hot pressing in a fiber/cristobalite interphase/mullite-cordierite matrix structure. In the critical grain size range, the shear stress-induced transformation behavior was evaluated by fiber push-out technique.

II. Experimental Procedure

In order to make amorphous-type β-cristobalite powder, a clear sol was prepared from Ludox AS-40 Colloidal silica (40 wt% suspension in water, Du Pont Chemicals, Wilmington, DE); $Al(NO_3)_3 \cdot 9H_2O$ (reagent grade, Aldrich Chemical Co., Milwaukee, WI) and $Ca(NO_3)_2 \cdot 4H_2O$ (reagent grade, Aldrich Chemical Co., Milwaukee, WI) in proportions with a final composition of $CaO \cdot 2Al_2O_3$:

$80SiO_2$.[11] After dissolving these reagents in DI water, a PVA solution, acting as a polymeric carrier, was added and the mixture was heated up to 120°C. The PVA solution was prepared from 5 wt% polyvinyl alcohol (PVA, degree of polymerization 1700, Air Products and Chemicals, Inc., Allentown, PA) dissolved in water. The amount of PVA to cation sources in the solution was adjusted in such a way that there were 4 times more positively charged valences of cations than the negatively charged functional ends of the organics.[10] As viscosity of the solution increased by evaporation of water, the mixture was vigorously stirred. The remaining water was then dried, transforming the gel into a porous solid. Finally, the precursor was ground and calcined at 1100°C for 1 hour. The calcined powder was attrition-milled with zirconia media for 1 hour at 180 rpm. Iso-propyl alcohol was used as a solvent for milling. 30 g of calcined powder was attrition-milled in a 1200 ml jar.

The dipping slip for fiber coating was prepared with 25 vol% amorphous-type β-cristobalite powder and 75 vol% water. 0.2 wt% (dry weight basis of powder) Darvan C (R. T. Vanderbilt Company, Inc.) and 0.1 wt% PVA solution (5 wt% PVA dissolved in water) were mixed to the slip as a deflocculant and binder, respectively. The mixture was ball milled with zirconia media for 6 hours. The matrix, consisting of 50 wt% mullite (KM Mullite-101 Kyotitsu, Nagoya, Japan) and 50 wt% cordierite (Baikalox 705G, Baikowski International Co.), was prepared by wet ball-milling the mixture for 12 hours and seiving the dried powder.

Amorphous-type β-cristobalite powder was dip-coated on to continuous mullite and sapphire fibers. The fibers were cut approximately into 15 mm long, cleaned by HF, and dip coated with β-cristobalite slurry. The thickness of coating was maintained at ~30 μm by repeated dipping and drying.

The fiber-containing pellets, which were made by uniaxially dry press, were loaded in a graphite die with compatible oxides surrounding the pressed materials, then hot pressed under an argon atmosphere at 28 MPa, at temperature of 1200°C for 1 hour. The specimens for push-out test were prepared by slicing perpendicular to the fiber direction. The thin sliced samples, which have a thickness of 0.8 mm, were polished and annealed at 1300°C for 10 hours. Push-out test was conducted in a universal testing machine (model 4502, Instron Corp., Canton, MA) to evaluate the interfacial properties of model composite. It is shown in Fig. 1. The testing was conducted using a constant crosshead speed of 1 μm/s. A load-displacement curve was recorded by a computer. The scanning electron microscopy (SEM, Hitachi S-530, Japan) was used to examine the debonded interface.

The specific surface area of the attrition-milled powder and the average grain size of the hot-pressed and annealed cristobalite were measured by nitrogen gas absorption (Model ASAP 2400, Micromeritics, Norcross, GA)

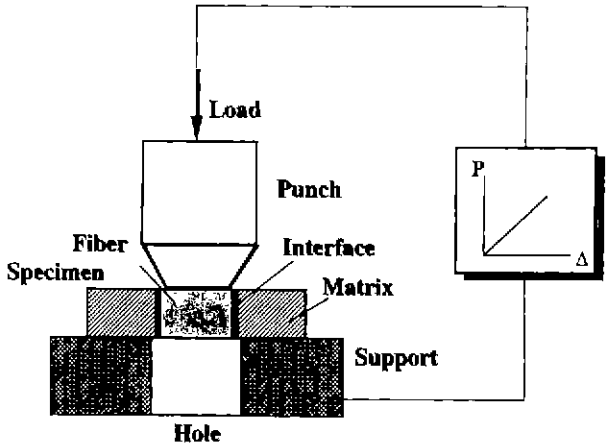

Fig. 1. The set-up of push-out test for model of interface system

and Jeffries-Saltykov method, respectively.[11] The phase change between α and β-cristobalite was studied using a Rigaku spectrometer (DMax automated powder diffractometer, Rigaku/USA, Danvers, MA) with CuKα radiation (40 kV, 40 mA).[11] The pellets for XRD analysis were hot-pressed and annealed with the same method as the fiber-containing pellet. The shear-induced transformation behavior was tested by grinding the annealed specimen on a 800 mesh SiC paper.

III. Results and Discussion

The attrition-milled, amorphous-type β-cristobalite powder had an average particle size and a BET specific surface area of 0.3 μm and 72 m^2/g, respectively.[11] The phase transformation behavior of polycrystalline β-cristobalite is listed in Table I. After hot pressing and annealing for 10 hours, the densified cristobalite, consisting of 61 vol% β-cristobalite and 39 vol% α-cristobalite, had an average grain size of 4.2 μm. Thermally-induced transformation, which occurred spontaneously on cooling, resulted in the formation of the α-cristobalite in the β-cristobalite matrix. However, microcracks were not accompanied by the transformation. After grinding the densified cristobalite, 13 vol% transformed to α-cristobalite through shear stress.

The result of fiber push-out test was represented by four individual steps. Stage I showed a linear elastic loading, followed by debonding in stage II. Stage III exhibited interphase sliding, and finally, stage IV revealed

Table 1. Shear-Induced Phase Transformation Behavior of Chemically Stabilized β-Cristobalite (Condition for Critical Grain Size: Hot press at 1200°C for 1 h and Annealing for 10 h at 1300°C)

Average grain size (μm)	Ratio of α/β phase (vol%)	Amount of shear-induced transformed α-Cristobalite by grinding (vol%)
4.2	β: 61 α: 39	13

the matrix crack and further sliding. Representative push-out curves for mullite and sapphire fiber systems are shown in Figs. 2 and 3. In the mullite fiber system, the load increased linearly with displacement until a critical load P1. At the critical load P1, the interfacial stress was large enough to produce a shear-induced phase transformation resulting in microcracks in the β-cristobalite coating layer which was observed by a volume decrease. The shear-induced transformation accompanying 3.2% volume decrease, which was estimated in Table 1, resulted in the microcracks in the cristobalite interphase. The debonding within the interphase decreased the critical load to P2, which is followed by a static friction increasing the load to P3 as seen in the push-out test of the SiC/SiAlON composite.[21] Over the maximum static friction, the fiber experienced frictional sliding. When the fiber slid to P4, the matrix at the bottom of the specimen was chipped due to the growth of the interphase cracks into matrix. Finally, the load dropped to P5. The fiber continuously slid out after P5.

The push-out curve for sapphire fiber is shown in Fig. 3. The debonding stress of sapphire fiber/β-cristobalite interphase was lower than that of the mullite fiber system. The difference was caused by a differential thermal

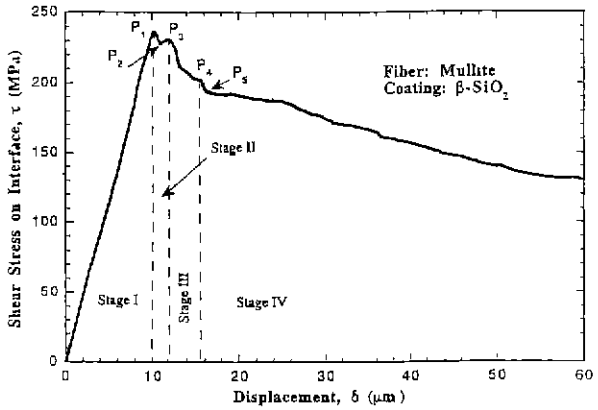

Fig. 2. Push-out load vs. displacement curve for mullite fiber/β-cristobalite interphase.

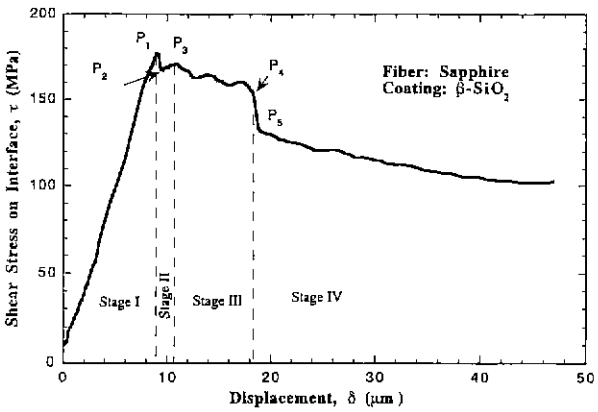

Fig. 3. Push-out load vs. displacement curve for sapphire fiber/β-cristobalite interphase.

expansion coefficient. The thermal expansion coefficient of sapphire fiber was $\sim 8\times10^{-6}$/°C,[22] which was much higher than the thermal expansion coefficient of β-cristobalite, $\sim 1.5\times10^{-6}$/°C.[11] When specimen was cooled down from hot-pressing and annealing, some residual tensile stress was induced in the interface resulting in the debonding within the interface between the sapphire fiber and the β-cristobalite interphase.

The length of stage III in the push-out test was quite different between the two fiber systems. In the sapphire fiber, it was ~8 μm, but only ~3 μm for mullite. This was caused by the different debonding mechanisms. The smoother debonding surface in sapphire fiber/β-cristobalite resulted in less microcracks in the β-cristobalite interphase in comparison to the mullite fiber/β-cristobalite system which had a debonding in the interphase. It was due to the longer progressive sliding length in the push-out test of the sapphire fiber.

The SEM micrographs identified the process in the fiber push-out. Fig. 4(a) shows the pushed-out fiber from the view of the mullite fiber/β-cristobalite bottom. The rough appearance was observed on the fiber surface, and the chip-out-characteristic existed in the matrix near the interphase. The thickness of interphase was approximate 25 μm. Fig 4(b) was the back scattering electron micrograph of a close up view of the interphase. The primary cracks were observed in both radial and circumferential directions. Several microcracks were also

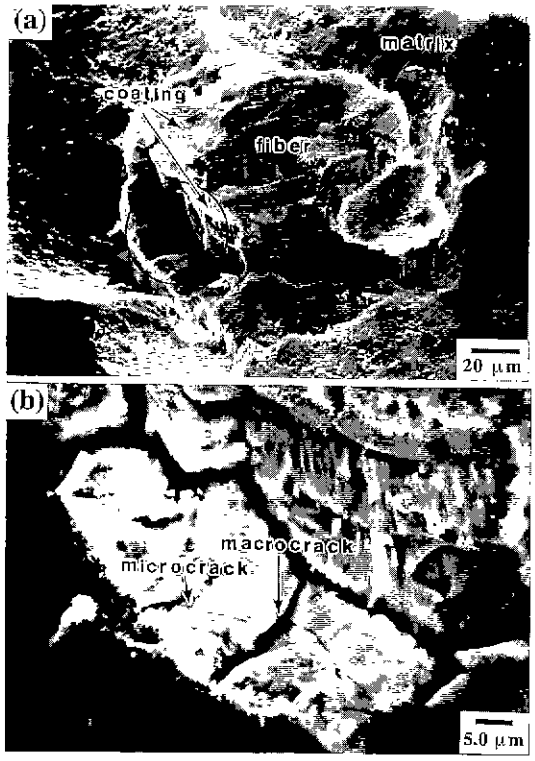

Fig. 4. (a) SEM photograph of mullite fiber/β-cristobalite interphase after push-out test and (b) its enlarged (circle region) back scattering electron image.

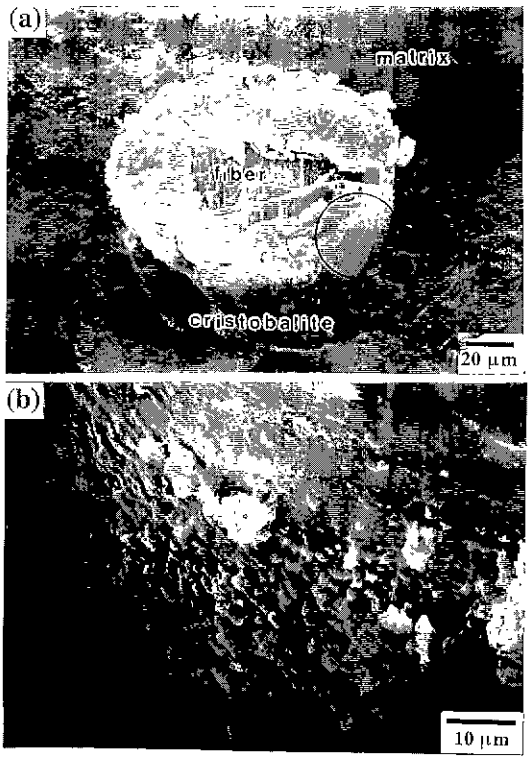

Fig. 5. (a) SEM photograph of sapphire fiber/β-cristobalite interphase after push-out test and (b) its enlarged photograph (circle region) for sapphire fiber surface.

observed in the interphase as indicated by the arrow. The same contrast between fiber surface and interphase indicated no difference in composition. This result meant that debonding occurred within the interphase, rather than the interface between the mullite fiber and β-cristobalite interphase. The SEM micrographs of sapphire fiber after push-out are shown in Fig. 5. The site of debonding and sliding was located at the interface between the sapphire fiber and the β-cristobalite interphase (Fig. 5(a)). Some pieces of cristobalite were observed on the smooth sapphire fiber surface in the electron micrograph (Fig. 5(b)).

IV. Conclusions

The $\beta \rightarrow \alpha$ phase transformation weakening behavior in the chemically stabilized β-cristobalite was observed by the fiber push-out technique. In a mullite fiber/cristobalite interphase/mullite-cordierite matrix structure, debonding occurred within the cristobalite interphase by fiber push-out test. The critical load, 230 MPa, for debonding resulted in primary and secondary microcracks in the cristobalite matrix. The microcracks were due to the $\beta \rightarrow \alpha$ phase transformation weakening by shear stress.

References

1. W. M. Kriven, "Possible Alternative Transformation Tougheners to Zirconia: Crystallographic Aspects," *J. Am. Ceram. Soc.*, **71**[12], 1022-30 (1988).
2. W. M. Kriven, "Displacive Phase Transformation and Their Applications in Structural Ceramics," *J. de Physique IV, Colloque* **C8**, 101-110 (1995)
3. W. J. Clegg, K. Kendall, N. M. Alford, D. Birchall and T. W. Button, "A Simple Way to Make Tough Ceramics," *Nature*, **347**, 455-57 (1990).
4. W. M. Kriven and S. J. Lee, "Phase Transformation Weakening Behavior of Chemically Stabilized β-cristobalite, Part II. Mullite/Cordierite Laminates with a β-Cristobalite Interphase," *J. Am. Ceram. Soc.*, submitted.
5. W. J. Clegg, "The Fabrication and Failure of Laminar Ceramic Composites," *Acta Metall.*, **40**[11], 3085-93 (1992).
6. P. E. D. Morgan and D. B. Marshall, "Ceramic Composites of Monazite and Alumina," *J. Am. Ceram. Soc.*, **78**[6], 1553-63 (1995)
7. D H Kuo, W. M. Kriven and T. J. Mackin, "Control of Interfacial Properties through Fiber Coating Monazite Coatings in Oxide/Oxide Composites," *J Am. Ceram, Soc.*, (1997), in press.
8. D. H. Kuo and W M. Kriven, "Fracture of Multilayer Oxide Composites," *J Mater. Sci. and Eng.*, (1997), in press.
9. W. M. Kriven, C. M. Huang, D Zhu, Y. Xu and S. C. Mirek. "Transformation Toughening of Titania Composites by Transformation Weakening of Enstatite Interphases," *J Am. Ceram. Soc*, to be published.
10. A F. Wright and A. J. Leadbetter, "The Structures of the β-cristobalite Phase of SiO_2 and $AlPO_4$," *Philos. Mag.*, **31**, 1391-401 (1975).
11. S. J Lee, "Characterization of Chemically Stabilized β-cristobalite Synthesized by Solution-Polymerization Route," *Kor. J. Ceram.*, **3**[2], 116-23 (1997).
12. D. A. Peacor, "High-Temperature Single-Crystal Study of the Cristobalite Inversion," *Z. Kristallogr.*, **138**, 274-98 (1973).
13. V. G. Hill and R. Roy, "Silica Structure Studies: V, The Variable Inversion in Cristobalite," *J. Am. Ceram. Soc.*, **41**[12], 532-37 (1958).
14. W. Eitel, "Structural Anomalies in Tridymite and Cristobalite." *Am. Ceram. Soc. Bull.*, **36**[4], 142-48 (1957).
15. M J Buerger, "Stuffed Derivatives of the Silica Structures," *Am. Mineral*, **39**[7-8], 600-14 (1954).
16. A. J. Perrotta, D. K. Grubbs, E. S. Martin and N. R. Dando. "Chemical Stabilization of β-cristobalite" *J. Am. Ceram. Soc.*, **72**[3], 441-47 (1989).
17. A. H. Heuer, N. Claussen, W. M. Kriven and M. Ruhle, "Stability of Tetragonal ZrO_2 Particles in Ceramic Matrices," *J. Am. Ceram. Soc.*, **65**[12], 642-50 (1982).
18. W. M. Kriven, C. J. Chan and E. A. Barinek, "The Particle-Size Effect of Dicalcium Silicate in a Calcium Zirconate Matrix"; pp 145-55 in Advances in Ceramics, Vol. 24, *Science and Technology of Zirconia III* Edited by S. Somiya, N. Yamamoto and H. Yanagida. American Ceramic Society, Westerville, OH, 1988.
19. C. J. Chan, W M. Kriven and J. F. Young, "Physical Stabilization of the $\beta \rightarrow \gamma$ Transformation in Dicalcium Silicate." *J. Am. Ceram. Soc.*, **75**[6], 1621-27 (1992).

20 C. M. Huang, D. H. Kuo, Y. J. Kim and W. M. Kriven, "Phase Stability of Chemically Derived Enstatite ($MgSiO_3$) Powders." *J. Am. Ceram Soc.*, **77**[10], 2625-31 (1994).
21. C. M. Huang, D. Zhu, Y. Xu and W. M. Kriven, "Interfacial Properties of SiC Monofilament Reinforced β-SiAlON Composites," *Mater. Sci. Eng.*, **A201**, 159-68 (1995)
22. Ceramic Source, Vol. 7, pp. 345. American Ceramic Society, Westerville, OH, 1991.